



# Fuzzy parametric uncertainty analysis of linear dynamical systems: A surrogate modeling approach

R. Chowdhury, S. Adhikari\*

College of Engineering, Swansea University, Singleton Park, Swansea SA2 8PP, UK

## ARTICLE INFO

### Article history:

Received 13 May 2011  
Received in revised form  
27 April 2012  
Accepted 3 May 2012  
Available online 2 June 2012

### Keywords:

Fuzzy systems  
Structural dynamics  
Uncertainty propagation  
HDMR

## ABSTRACT

Uncertainty propagation engineering systems possess significant computational challenges. This paper explores the possibility of using correlated function expansion based metamodelling approach when uncertain system parameters are modeled using Fuzzy variables. In particular, the application of High-Dimensional Model Representation (HDMR) is proposed for fuzzy finite element analysis of dynamical systems. The HDMR expansion is a set of quantitative model assessment and analysis tools for capturing high-dimensional input–output system behavior based on a hierarchy of functions of increasing dimensions. The input variables may be either finite-dimensional (i.e., a vector of parameters chosen from the Euclidean space  $\mathfrak{R}^M$ ) or may be infinite-dimensional as in the function space  $C^M[0, 1]$ . The computational effort to determine the expansion functions using the alpha cut method scales polynomially with the number of variables rather than exponentially. This logic is based on the fundamental assumption underlying the HDMR representation that only low-order correlations among the input variables are likely to have significant impacts upon the outputs for most high-dimensional complex systems. The proposed method is integrated with a commercial Finite Element software. Modal analysis of a simplified aircraft wing with Fuzzy parameters has been used to illustrate the generality of the proposed approach. In the numerical examples, triangular membership functions have been used and the results have been validated against direct Monte Carlo simulations.

© 2012 Elsevier Ltd. All rights reserved.

## 1. Introduction

The consideration of uncertainties in numerical models to obtain the variability of vibration response is becoming more desirable for industrial scale finite element models. Broadly speaking, there are two aspects to this problem. The first is the quantification of parametric and/or non-parametric uncertainties associated with the model and the second is the propagation of uncertainties through the model. This paper is concerned with the second problem. Several types of uncertainties can exist in a physics based computational model. Such uncertainties include, but are not limited to (a) parameter uncertainty (e.g., uncertainty in geometric parameters, friction coefficient, strength of the materials involved); (b) model uncertainty (arising from the lack of scientific knowledge about the model which is *a priori* unknown); and (c) experimental error (uncertain and unknown errors percolate into the model when they are calibrated against experimental results). These uncertainties must be assessed and managed for credible computational predictions.

\* Corresponding author. Tel.: +44 1792 602088; fax: +44 1792 295676.

E-mail addresses: [R.Chowdhury@swansea.ac.uk](mailto:R.Chowdhury@swansea.ac.uk) (R. Chowdhury), [S.Adhikari@swansea.ac.uk](mailto:S.Adhikari@swansea.ac.uk) (S. Adhikari).

When substantial statistical information exists, the theory of probability and stochastic processes offer a rich mathematical framework to represent such uncertainties. In a probabilistic setting, the data (parameter) uncertainty associated with the system parameters, such as the geometric properties and constitutive relations (i.e., Young's modulus, mass density, Poisson's ratio, damping coefficients), can be modeled as random variables or stochastic processes using the so-called parametric approach. These uncertainties can be quantified and propagated, for example, using the stochastic finite element method [1–4]. The reliable application of probabilistic approaches requires information to construct the probability density functions of uncertain parameters. This information may not be easily available for many complex practical problems. In such situations, non-probabilistic approaches, such as interval algebra [5], convex models [6] and fuzzy set [7] based methods, can be used. In this paper the uncertain variables describing the system parameters are modeled using fuzzy variables.

Over the past decade, significant developments have taken place in fuzzy finite element analysis of linear dynamical systems (see, for example, the review papers [8–10]). A fuzzy variable can be viewed as a generalization of an interval variable. When an uncertain variable is modeled using the interval approach, the values of the variable lie within a lower and an upper bound. The fuzzy approach generalizes this concept by introducing a membership function. In the context of computational mechanics, the aim of a fuzzy finite element analysis is to obtain the range of certain output quantities (such as displacement, acceleration and stress) given the membership of data in the set of input variables. This problem, known as the uncertainty propagation problem, has taken center stage in recent research activities in the field. In principle, an uncertainty propagation problem can be always solved using the so-called direct Monte Carlo simulation. Using this approach, a large number of members of the parameter set are individually simulated and bounds are obtained from the resulting outputs. For most practical problems, direct Monte Carlo simulation is prohibitively computationally expensive. Therefore, the aim of the majority of current research is to reduce the computational cost. Since fuzzy variables are a generalization of interval variables, methods applicable for interval variables, such as classical interval arithmetic [5], affine analysis [11,12] or vertex theorems [13], can be used. The Neumann expansion [14], the transformation method [15–18], and more recently, response surface based methods [19,20] have been proposed for fuzzy uncertainty propagation. In the context of dynamical systems, several authors have extended classical modal analysis to fuzzy modal analysis [21–27].

A crucial factor in the efficiency of all the methods is the number of input variables, often known as the 'dimensionality' of the problem. Here we investigate the use of the High-Dimensional Model Representation (HDMR) approach [28] to address this issue. The HDMR expansion is an efficient formulation for high-dimensional mapping in complex systems if the higher order variable correlations are weak, thereby permitting the input–output relationship behavior to be captured by the terms of low-order. The computational effort to determine the expansion functions using the  $\alpha$ -cut method will scale polynomially with the number of variables rather than exponentially. This logic is based on the fundamental assumption underlying the HDMR representation that only low-order correlations among the input variables are likely to have significant impacts upon the outputs for most high-dimensional complex systems. HDMR expansions can be broadly categorized as RS (Random Sampling)-HDMR and Cut-HDMR. In the first case, the component functions are determined by integrating over randomly scattered sample points. Whereas the component functions in Cut-HDMR expansion are evaluated along lines or planes or volumes (i.e., cuts) with respect to a reference point in sample space.

Recently, authors have developed the HDMR-based fuzzy finite element method for uncertain dynamical system [29], where HDMR was constructed based on regularized samples and conditional responses at selected sample points. Following are the distinctive features of the present approach: (i) randomly scattered sample points are chosen from input space, rather than along lines or planes or volumes (i.e., cuts) with respect to a reference point in sample space, (ii) sample points are generated using Sobol's sequence [30,31], and (iii) different analytical basis functions, including orthonormal polynomials, cubic B splines, and polynomials for approximating the RS-HDMR component functions can be used. The outline of the paper is as follows. Section 2 gives a brief background of fuzzy variables. Structural dynamic analysis with fuzzy parametric uncertain variables is discussed in Section 3. The proposed high-dimensional model representation approach is described in Section 4. Three numerical examples illustrating the proposed method is given in Section 5. The method is then integrated with a commercial Finite Element (FE) software. In the numerical examples, triangular membership functions have been used and the results have been validated against direct Monte Carlo simulations. Based on the studies in the paper, conclusions are drawn in Section 6.

## 2. A brief overview of fuzzy variables

The mathematical description of fuzzy variables can be given in various levels of abstraction. The easiest way to describe a fuzzy variable is via interval variables. A scalar interval variable  $x^l$  can be defined as

$$x^l = [x_l, x_h] = \{x \in \mathbb{R} \mid x_l \leq x \leq x_h\} \quad (1)$$

The scalar interval variable can be extended to vector- and tensor-valued variables in a natural way. In contrast to the probabilistic description, the entries of a vector or tensor are always considered to be uncorrelated. Therefore, generalizing (1), a  $n$ -dimensional interval vector simply lies within a  $n$ -dimensional hypercube in  $\mathbb{R}^n$ . The concept of the fuzzy set was proposed by Zadeh [7] to represent imprecise information in a mathematically rigorous manner. Since then numerous books and papers have discussed the detail of fuzzy sets (see, for example, the review papers [8–10]).

A fuzzy set can be defined by extending the deterministic (crisp) value and combining interval algebra. Suppose  $X$  is a (real) space whose elements are denoted by  $x$ . The key idea in fuzzy set theory is the membership function  $\mu_{\tilde{A}} : X \rightarrow M \subseteq [0, 1]$  which maps  $X$  into the membership space  $M$ . If  $\mu_{\tilde{A}}(x) = 1$ , then  $x$  is definitely a member of the fuzzy set  $\tilde{A}$ . On the other hand, if  $\mu_{\tilde{A}}(x) = 0$ , then  $x$  is definitely not a member of the fuzzy set  $\tilde{A}$ . For any intermediate case  $0 < \mu_{\tilde{A}}(x) < 1$ , the membership is uncertain. Therefore, using the membership function, a fuzzy set can be defined as

$$\tilde{A} = \{(x, \mu_{\tilde{A}}(x)) | x \in X\} \tag{2}$$

If  $\sup_{x \in X} \mu_{\tilde{A}}(x) = 1$ , then the fuzzy set  $\tilde{A}$  is called normal. In this paper only normalized fuzzy sets are considered.

The notion of support and  $\alpha$ -cuts of a fuzzy set play a crucial role in the computational and analytical methods involving fuzzy sets. The support of a fuzzy set  $\tilde{A}$  is the crisp set of all  $x \in X$ , such that  $\mu_{\tilde{A}}(x) > 0$ , or mathematically

$$\text{supp}(\tilde{A}) = \{x | \mu_{\tilde{A}}(x) > 0, x \in X\} \tag{3}$$

The  $\alpha$ -cut or  $\alpha$ -level set of  $\tilde{A}$  is the crisp set  $A_\alpha$  such that

$$A_\alpha = \{x | \mu_{\tilde{A}}(x) \geq \alpha, x \in X, 0 < \alpha \leq 1\} \tag{4}$$

In the case of bounded supports, we also define the 0-cut as the largest closed interval  $A_0 = [\inf(\text{supp}(\tilde{A})), \sup(\text{supp}(\tilde{A}))]$ . Often  $\alpha$ -cuts are considered as intervals of confidence, since in case of convex fuzzy sets, they are closed intervals associated with a gradation of confidence between  $[0, 1]$ .

### 3. Fuzzy uncertainty propagation in structural dynamics

The equation of motion of a damped  $n$ -degree-of-freedom linear structural dynamical system with fuzzy parameters can be expressed as

$$\mathbf{M}(\mathbf{x})\ddot{\mathbf{q}}(t) + \mathbf{C}(\mathbf{x})\dot{\mathbf{q}}(t) + \mathbf{K}(\mathbf{x})\mathbf{q}(t) = \mathbf{p}(t) \tag{5}$$

where  $\mathbf{x} \in \mathbb{R}^M$  is a fuzzy vector,  $\mathbf{p}(t) \in \mathbb{R}^n$  is the forcing vector,  $\mathbf{q}(t) \in \mathbb{R}^n$  is the response vector and  $\mathbf{M} \in \mathbb{R}^{n \times n}$ ,  $\mathbf{C} \in \mathbb{R}^{n \times n}$  and  $\mathbf{K} \in \mathbb{R}^{n \times n}$  are the mass, damping and stiffness matrices, respectively. When fuzzyness in the system parameters, boundary conditions and geometry are considered, the system matrices become matrices with fuzzy entries. Uncertainties in system (5) are completely characterized by the membership functions of the entries of the vector  $\mathbf{x}$ . The main interests in structural dynamic analysis are (a) quantification of uncertainty in the eigenvalues and eigenvectors and (b) quantification of uncertainty in the response  $\mathbf{q}$  either in the time domain or in the frequency domain. Few researchers [20–22] have considered uncertainty quantification in the frequency response function of a linear dynamical systems with fuzzy variables. This problem, in effect, has to solve the uncertainty propagation problem, which can be expressed in a general way as

$$\mathbf{y} = \mathbf{f}(\mathbf{x}) \in \mathbb{R}^m \tag{6}$$

where  $\mathbf{f}(\bullet) : \mathbb{R}^M \rightarrow \mathbb{R}^m$  is a smooth nonlinear function of the input fuzzy vector  $\mathbf{x}$ . The function  $\mathbf{f}(\bullet)$  can be the frequency response function of Eq. (5) or the eigensolutions.

The uncertainty propagation of fuzzy variables through smooth nonlinear functions can be performed using interval algebra based approach or global optimisation based approach. In the interval algebra based approach, a fuzzy variable is considered as an interval variable for each  $\alpha$ -cut and propagated using classical interval arithmetic [5]. Unless the functions are simple and the number of variables is small, this approach produces a very large bound for the output variables. Such overestimates may not be useful for practical design decisions. While for the global optimisation based approach, for each  $\alpha$ -cut two optimisation problems are solved for each of the output quantities. The first optimisation problem aims to find the minimum value, while the second optimisation problem aims to find the maximum value of the output quantity. By combining results for all  $\alpha$ -cuts, one can obtain the fuzzy description of the output quantities. The advantage of this approach is that the bounds are ‘tight’ and the wealth of tools are available for mathematical optimisation can be employed in a reasonably straight-forward manner. The disadvantage is, of course, the computational cost as two optimisation problems need to be solved for every  $\alpha$ -cut and for every output quantity. For these reasons, efficient numerical methods are necessary to use this approach. In this paper the global optimisation based approach is adopted for uncertainty propagation.

For linear structural dynamic problems, typically one is interested in dynamic response in the time or frequency domain. The fuzzy eigenvalue problem corresponding to dynamical system (5) can be expressed as

$$\mathbf{K}(\mathbf{x})\phi_j(\mathbf{x}) = \omega_j(\mathbf{x})^2 \mathbf{M}(\mathbf{x})\phi_j(\mathbf{x}) \quad \forall j = 1, \dots, n \tag{7}$$

here  $\omega_j(\mathbf{x})$  and  $\phi_j(\mathbf{x})$  are  $j$ th fuzzy natural frequency and mode shape of system. Assuming the system is proportionally damped, the fuzzy displacement response in the frequency domain with zero-initial conditions can be expressed in terms of fuzzy eigenvalues and eigenvectors as

$$\bar{\mathbf{q}}(\mathbf{x}, \omega) = \sum_{j=1}^n \frac{\phi_j(\mathbf{x})^T \bar{\mathbf{p}}(\omega)}{-\omega^2 + 2i\omega\zeta_j\omega_j(\mathbf{x}) + \omega_j(\mathbf{x})^2} \phi_j(\mathbf{x}) \tag{8}$$

here  $\bar{\mathbf{q}}(\omega)$  and  $\bar{\mathbf{p}}(\omega)$  are, respectively, the Fourier transforms of  $\mathbf{q}(t)$  and  $\mathbf{p}(t)$ . In the time domain, the displacement response of system (5) can be expressed as

$$\mathbf{q}(t) = \sum_{j=1}^n \left\{ \int_0^t \frac{1}{\omega_{d_j}(\mathbf{x})} \phi_j(\mathbf{x})^T \mathbf{f}(\tau) e^{-\zeta_j \omega_j(\mathbf{x})(t-\tau)} \sin(\omega_{d_j}(\mathbf{x})(t-\tau)) d\tau \right\} \phi_j(\mathbf{x}) \quad (9)$$

where the damped natural frequencies are given by

$$\omega_{d_j}(\mathbf{x}) = \omega_j(\mathbf{x}) \sqrt{1 - \zeta_j^2} \quad (10)$$

For many practical applications, linear or nonlinear transformations of fuzzy eigensolutions and displacement response can be of interest.

Here we formulate the optimisation problem in the time domain. But the same formulation also applies to the frequency domain response with minor modifications arising due to the fact that the frequency domain response is complex in nature.

Suppose  $I$  is the set of integers and  $r \in I$  is the number of  $\alpha$ -cuts used for each of the input fuzzy variables  $x_j$ ,  $j = 1, 2, \dots, m$ , in the numerical analysis. Therefore,  $0 \leq [\alpha_1, \alpha_2, \dots, \alpha_r] < 1$  are the values of  $\alpha$  for which we wish to obtain our outputs. Suppose  $f_j(\mathbf{x}_{z_k})$ ,  $j = 1, 2, \dots, M$ , are the functions which relate the output  $y_{jk}$  with the interval variable  $\mathbf{x}_{z_k}$  associated with  $\alpha_k$  for some  $k \leq r$  such that

$$y_{jk}(t) = f_j(\mathbf{x}_{z_k}, t), \quad j = 1, 2, \dots, m, \quad k = 1, 2, \dots, r \quad \forall t \quad (11)$$

The fuzzy uncertainty propagation problem can be formally defined as the solution of the following set of optimisation problems:

$$\left. \begin{aligned} y_{jk_{\min}}(t) &= \min(f_j(\mathbf{x}_{z_k}, t)) \\ y_{jk_{\max}}(t) &= \max(f_j(\mathbf{x}_{z_k}, t)) \end{aligned} \right\} \quad \forall j = 1, 2, \dots, m, \quad k = 1, 2, \dots, r \quad \forall t \in [0, T] \quad (12)$$

where  $[0, T]$  denotes the time interval of interest. In total, there are  $2mr$  optimisation problems of every time instant used in the numerical procedure. The computational cost of each of these optimisation problems depends on the dimensionality of the  $\mathbf{x}_{z_k}$ , that is,  $M$ . Since  $m$ ,  $r$ ,  $t$ , and  $M$  are fixed by the problem, there are two ways to reduce the computational cost, namely (a) to reduce the number of function evaluations by using superior optimisation techniques or (b) to reduce the cost of each function evaluation, for example, by 'replacing' the expensive function by a surrogate model. De Munck et al. [32] used a Kriging based approach. Adhikari et al. [29] proposed a basic HDMR approach. Clearly, if the cost of each function evaluation can be reduced, then the overall computational cost to solve the uncertainty propagation problem will be reduced no matter what optimisation algorithm is used. Here we explore a random sampling based HDMR approach to efficiently generate the surrogate model. The aim is to 'build' the surrogate model with the minimum number of evaluations of the original function. Once the surrogate model is obtained, Monte Carlo simulation is used to obtain the minimum and maximum of the function.

## 4. High-dimensional model representation (HDMR)

### 4.1. Background

The basic High-Dimensional Model Representation (HDMR) for systems Fuzzy uncertain variable was proposed by the authors [29]. In this section we briefly review the ordered sampling based HDMR and consequently the new randomly sampled HDMR (RS-HDMR). HDMR of an arbitrary  $M$ -dimensional function  $f(\mathbf{x})$ ,  $\mathbf{x} \in \mathbb{R}^M$  can be derived by partitioning the identity operator  $\mathcal{I}$ , called  $\mathcal{I}_M$  in the  $M$ -dimensional case and also in the 1D case hereafter, with respect to the projectors  $\mathcal{P}_1, \mathcal{P}_2, \dots, \mathcal{P}_M$ . This can be expressed as follows [33–40]:

$$\begin{aligned} \mathcal{I}_M &= \prod_{m=1}^M (\mathcal{P}_m + (\mathcal{I}_1 - \mathcal{P}_m)) = \underbrace{\prod_{m=1}^M \mathcal{P}_m}_{1 \text{ term}} + \underbrace{\sum_{m=1}^M (\mathcal{I}_1 - \mathcal{P}_m) \prod_{s \neq m} \mathcal{P}_s}_{\binom{M}{1} \text{ terms}} + \underbrace{\sum_{m=1}^M \sum_{s=m+1}^M (\mathcal{I}_1 - \mathcal{P}_m)(\mathcal{I}_1 - \mathcal{P}_s) \prod_{p \neq m, s} \mathcal{P}_p}_{\binom{M}{2} \text{ terms}} \\ &+ \dots + \underbrace{\sum_{m=1}^M \mathcal{P}_m \prod_{s \neq m} (\mathcal{I}_1 - \mathcal{P}_s)}_{\binom{M}{M-1} \text{ terms}} + \underbrace{\prod_{m=1}^M (\mathcal{I}_1 - \mathcal{P}_m)}_{1 \text{ term}} \end{aligned} \quad (13)$$

composed of  $2^M$  mutually orthogonal terms. The orthogonal representation of Eq. (13) is a manifestation of the HDMR and can be rewritten as [41,42]

$$f(\mathbf{x}) = f_0 + \sum_{i=1}^M f_i(x_i) + \sum_{1 \leq i < j \leq M} f_{ij}(x_i, x_j) + \dots + f_{123 \dots M}(x_1, x_2, \dots, x_M) = \sum_{l=0}^M \eta_l(\mathbf{x}) \quad (14)$$

where  $f_0$  is a constant term representing the zeroth-order component function or the mean response of any response function  $f(\mathbf{x})$ .  $f_i$  is the first-order term expressing the effect of variable  $x_i$  acting alone upon the output  $f(\mathbf{x})$ , and this function is generally nonlinear. The function  $f_{ij}(x_i, x_j)$  is a second-order term which describes the cooperative effects of the variables  $x_i$  and  $x_j$  upon the response. The higher order terms give the cooperative effects of increasing numbers of input variables acting together to influence the output. The last term  $f_{123\dots M}(x_1, x_2, \dots, x_M)$  contains any residual dependence of all the input variables locked together in a cooperative way to influence the output. Once all the relevant component functions in Eq. (14) are determined and suitably represented, then the component functions constitute the HDMR, thereby replacing the original computationally expensive method of calculating the response by the computationally efficient meta model. Usually, the higher order terms in Eq. (14) are negligible [28] such that an HDMR with only a few low order correlations among the input variables is adequate to describe the output behavior. This in turn results in rapid convergence of the HDMR expansion [35,36], which has a finite number of terms and is always exact [28,39] in the least-square senses. Other popular expansions (e.g., polynomial chaos) have been suggested [1], but they commonly have an infinite number of terms with some specified functions, such as Hermite polynomials [39]. HDMR expansions can be broadly categorized as RS (Random Sampling)-HDMR and Cut-HDMR. In the first case, the component functions are determined by integrating over randomly scattered sample points. Whereas the component functions in Cut-HDMR expansion are evaluated along lines or planes or volumes (i.e., cuts) with respect to a reference point in sample space.

#### 4.2. Cut-HDMR

When an ordered sampling technique is used in order to evaluate the response, it is known as Cut-HDMR expansion. To generate the HDMR approximation of any function, more precisely the cut-center based HDMR, first a reference point  $\bar{\mathbf{x}} = (\bar{x}_1, \bar{x}_2, \dots, \bar{x}_M)$  has to be defined in the variable space. In the convergence limit, where all correlated functions in Eq. (14) are considered, the cut-HDMR is invariant to the choice of reference point  $\bar{\mathbf{x}}$ . However, in practice, the choice of reference point  $\bar{\mathbf{x}}$  is important for the cut-HDMR, especially if only the first few terms, say up to first- and second-order, in Eq. (14) are considered [43]. Sobol [35] showed that the reference point  $\bar{\mathbf{x}}$  at the middle of the input domain appears to be the optimal choice. The expansion functions are determined by evaluating the input-output responses of the system relative to the defined reference point along the associated lines, surfaces or sub-volumes in the input variable space. This process reduces to the following relationship for the component functions in Eq. (14):

$$\begin{aligned}
 f_0 &= \int dx f(\mathbf{x}) \\
 f_i(x_i) &= \int dx^i f(\mathbf{x}) - f_0 \\
 f_{ij}(x_i, x_j) &= \int dx^{ij} f(\mathbf{x}) - f_i(x_i) - f_j(x_j) - f_0
 \end{aligned}
 \tag{15}$$

where  $\int dx^i$  means to integrate over all  $M$  variables except  $x_i$  and  $\int dx^{ij}$  means to integrate over all  $M$  variables except  $x_i$  and  $x_j$ , etc. These integrals are generally evaluated using numerical integration techniques. Substituting the component functions defined in Eq. (15) into Eq. (14), the general expression of the cut-HDMR can be expressed as

$$\begin{aligned}
 f(\mathbf{x}) &= \sum_{1 \leq i_1 < \dots < i_\beta \leq M} f(x_{i_1}, \dots, x_{i_\beta}; \bar{x}^{i_1, \dots, i_\beta}) - (M-\beta) \sum_{1 \leq i_1 < \dots < i_{\beta-1} \leq M} f(x_{i_1}, \dots, x_{i_{\beta-1}}; \bar{x}^{i_1, \dots, i_{\beta-1}}) \\
 &+ \frac{(M-\beta+1)!}{2!(M-\beta-1)!} \sum_{1 \leq i_1 < \dots < i_{\beta-2} \leq M} f(x_{i_1}, \dots, x_{i_{\beta-2}}; \bar{x}^{i_1, \dots, i_{\beta-2}}) - \dots \mp \frac{(M-2)!}{(\beta-1)!(M-\beta-1)!} \sum_{1 \leq i \leq M} f(x_i; \bar{x}^i) \\
 &\pm \frac{(M-1)!}{\beta!(M-\beta-1)!} \sum_{1 \leq i \leq M} f(\bar{\mathbf{x}})
 \end{aligned}
 \tag{16}$$

where  $\beta$  is the order of the cut-HDMR approximation,  $1 \leq \beta \leq (M-1)$  and the  $+$  or  $-$  sign of the last term in Eq. (16) corresponds to  $\beta$  being even or odd, respectively. Considering the weak role of the higher-order correlation effects, the approximation is likely to converge at a lower cut-HDMR order, say,  $\beta \ll M$ . The particular form of Eq. (16) for  $\beta = 1, 2$  or  $3$  corresponds to first-, second- or third-order cut-HDMR can be explicitly given as

$$\hat{f}(\mathbf{x}) = \sum_{1 \leq i \leq M} f(x_i; \bar{x}^i) - (M-1)f(\bar{\mathbf{x}}), \quad \beta = 1
 \tag{17}$$

$$\hat{f}(\mathbf{x}) = \sum_{1 \leq i < j \leq M} f(x_i, x_j; \bar{x}^{i,j}) - (M-2) \sum_{1 \leq i \leq M} f(x_i; \bar{x}^i) + \frac{(M-1)!}{2!(M-3)!} \sum_{1 \leq i \leq M} f(\bar{\mathbf{x}}), \quad \beta = 2
 \tag{18}$$

$$\hat{f}(\mathbf{x}) = \sum_{1 \leq i < j < k \leq M} f(x_i, x_j, x_k; \bar{x}^{i,j,k}) - (M-3) \sum_{1 \leq i < j \leq M} f(x_i, x_j; \bar{x}^{i,j}) + \frac{(M-2)!}{2!(M-4)!} \sum_{1 \leq i \leq M} f(x_i; \bar{x}^i) + \frac{(M-1)!}{3!(M-4)!} \sum_{1 \leq i \leq M} f(\bar{\mathbf{x}}), \quad \beta = 3
 \tag{19}$$

The term  $f(x_i; \bar{x}^i)$  is a function of the single  $x_i$  component (i.e., a cut along  $x_i$  through the reference point in the function space), while the other variables,  $x_j \equiv \bar{x}_j$ ,  $j \neq i$ , are fixed at the reference point. In the same manner,  $f(x_i, x_j; \bar{x}^{ij})$  is the observed response for all the variables,  $x_k \equiv \bar{x}_k$ ,  $k \neq i, j$ , fixed at the cut center except for  $x_i$  and  $x_j$ . A similar interpretation would apply to higher order cut-HDMR terms.

The notion of first-, second-order, etc. used in the HDMR does not imply the terminology commonly used either in the Taylor series or in the conventional polynomial based approximation formulae. In HDMR-based approximation, these terminologies are used to define the constant term, or for example, terms with one variable or two variables only. It is recognized that the lower order (e.g., first-order or second-order) function expansions in the HDMR, do not generally translate to linear or quadratic functions [36]. Each of the lower-order terms in the HDMR is sub-dimensional, but they are not necessarily low degree polynomials. The computational savings afforded by the HDMR are easily estimated. If the HDMR converges at  $\beta$  order with acceptable accuracy and considering  $s$  sample points for each variable, then the total number of numerical analyses needed to determine the HDMR is  $\sum_{k=0}^{\beta} [M!/k!(M-k)!(s-1)^k]$ .

#### 4.3. RS-HDMR

Distinct, but formally equivalent, HDMR expansions, all of which have the same structure as Eq. (14), may be constructed. When data are considered as randomly sampled, RS-HDMR [28,34] can be obtained. For RS-HDMR, we first rescale the variables  $x_i$  by some suitable transformations such that  $0 \leq x_i \leq 1$  for all  $i$ . The output function  $f(\mathbf{x})$  is then defined in the unit hypercube [28]

$$K^M = \{(x_1, x_2, \dots, x_M) / 0 \leq x_i \leq 1, i = 1, 2, \dots, M\} \quad (20)$$

The component functions of RS-HDMR possess the following forms [28,34]:

$$\begin{aligned} f_0 &= \int_{K^M} f(\mathbf{x}) d\mathbf{x} \\ f_i(x_i) &= \int_{K^{M-1}} f(\mathbf{x}) d\mathbf{x}^i - f_0 \\ f_{ij}(x_i, x_j) &= \int_{K^{M-2}} f(\mathbf{x}) d\mathbf{x}^{ij} - f_i(x_i) - f_j(x_j) - f_0 \end{aligned} \quad (21)$$

where  $d\mathbf{x}^i$  and  $d\mathbf{x}^{ij}$  are just the product  $dx_1 dx_2 \dots dx_M$  without  $dx^i$  and  $dx^{ij}$ , respectively. Finally, the last term  $f_{123\dots M}(x_1, x_2, \dots, x_M)$  is determined from the difference between  $f(x)$  and all the other component functions in Eq. (14). The RS-HDMR component functions satisfy the following condition: the integral of a component function of RS-HDMR with respect to any of its own variables is zero, i.e.

$$\int_0^1 f_{i_1 i_2 \dots i_l}(x_{i_1}, x_{i_2}, \dots, x_{i_l}) dx_s = 0, \quad s \in \{i_1, i_2, \dots, i_l\} \quad (22)$$

which defines the orthogonality relation between two RS-HDMR component functions as

$$\int_{K^M} f_{i_1 i_2 \dots i_l}(x_{i_1}, x_{i_2}, \dots, x_{i_l}) f_{j_1 j_2 \dots j_l}(x_{j_1}, x_{j_2}, \dots, x_{j_l}) d\mathbf{x} = 0 \quad \{i_1, i_2, \dots, i_l\} \neq \{j_1, j_2, \dots, j_l\} \quad (23)$$

The component functions  $f_i(x_i)$ ,  $f_{ij}(x_i, x_j)$ , ... are typically provided numerically, at discrete values of the input variables  $x_i$ ,  $x_j$ , ... produced from sampling the output function  $f(\mathbf{x})$  for employment on the right-hand side (rhs) of Eq. (21). Thus, numerical data tables can be constructed for these component functions, and the approximate value of  $f(\mathbf{x})$  for an arbitrary point  $\mathbf{x}$  can be determined from these tables by performing only low-dimensional interpolation over  $f_i(x_i)$ ,  $f_{ij}(x_i, x_j)$ , ... . To construct the numerical data tables for the RS-HDMR component functions [28,34], one needs to evaluate the above integrals. Evaluation of the high-dimensional integrals in the RS-HDMR expansion may be carried out by Monte Carlo random sampling. For instance,  $N$  samples of the  $M$ -dimensional vector  $\mathbf{x}^{(s)} = (x_1^{(s)}, x_2^{(s)}, \dots, x_M^{(s)})$  ( $s = 1, 2, \dots, N$ ) are randomly generated uniformly in  $K^M$ , and then  $f_0$  is approximated by the average value of  $f(\mathbf{x})$  at all  $\mathbf{x}^{(s)}$ :

$$f_0 = \int_{K^M} f(\mathbf{x}) d\mathbf{x} \approx \frac{1}{N} \sum_{s=1}^N f(\mathbf{x}^{(s)}) \quad (24)$$

When  $N \rightarrow \infty$ , an accurate value of  $f_0$  can be obtained. Very often the integrals converge quite fast, and a modest value of  $N$  may give a very good result. Moreover, the approximation of an integral by Monte Carlo sampling often does not depend significantly on the dimension  $M$ . This property is extremely beneficial for high-dimension systems. Direct determination of all RS-HDMR component functions [28,34] at different values of  $x_i$ ,  $x_j$ , ... by Monte Carlo integration requires a large number of random samples. For example, to determine  $f_i(x_i)$ , different sets of samples of  $f(x_i, \mathbf{x}^i)$  at  $(x_i, \mathbf{x}^i)^{(s)} = (x_1^{(s)}, x_2^{(s)}, \dots, x_{i-1}^{(s)}, x_i^{(s)}, x_{i+1}^{(s)}, \dots, x_M^{(s)})$  with distinct fixed values of  $x_i$  are needed, i.e.

$$f_i(x_i) = \int_{K^{M-1}} f(\mathbf{x}) d\mathbf{x}^i - f_0 \approx \frac{1}{N} \sum_{s=1}^N f(x_i, \mathbf{x}^i)^{(s)} - \frac{1}{N} \sum_{s=1}^N f(\mathbf{x}^{(s)}) \quad (25)$$

If  $x_i$  takes  $m$  distinct values, then  $mN$  samples are necessary to construct the  $f_i(x_i)$  numerical table. Similarly, to construct the  $f_{ij}(x_i, x_j)$  numerical table, different sets of samples of  $f(x_i, x_j, \mathbf{x}^{ij})$  at  $(x_i, x_j, \mathbf{x}^{ij})^{(s)} = (x_1^{(s)}, x_2^{(s)}, \dots, x_{i-1}^{(s)}, x_i^{(s)}, x_{i+1}^{(s)}, \dots, x_{j-1}^{(s)}, x_j^{(s)}, x_{j+1}^{(s)}, \dots, x_M^{(s)})$  with distinct fixed values of  $x_i, x_j$  are needed, i.e.

$$f_{ij}(x_i, x_j) = \int_{K^{M-2}} f(\mathbf{x}) d\mathbf{x}^{ij} - f_i(x_i) - f_j(x_j) - f_0 \approx \frac{1}{N} \sum_{s=1}^N f(x_i, x_j, \mathbf{x}^{ij})^{(s)} - \frac{1}{N} \sum_{s=1}^N f((x_i, \mathbf{x}^i)^{(s)}) - \frac{1}{N} \sum_{s=1}^N f((x_j, \mathbf{x}^j)^{(s)}) \tag{26}$$

$$+ \frac{1}{N} \sum_{s=1}^N f(\mathbf{x}^{(s)}) \tag{27}$$

If both  $x_i$  and  $x_j$  take  $m$  distinct values, then  $m^2N$  random samples are necessary to construct the  $f_{ij}(x_i, x_j)$ . The required number of samples increases exponentially with the order of the required RS-HDMR component functions. Thus, the direct approach is prohibitively expensive for the construction of high-order RS-HDMR component functions. To reduce the sampling effort, the RS-HDMR component functions are approximated by expansions in terms of a suitable set of basis functions, such as orthonormal polynomials

$$f_i(x_i) \approx \sum_{r=1}^k \alpha_r^i \varphi_r(x_i)$$

$$f_{ij}(x_i, x_j) \approx \sum_{p=1}^l \sum_{q=1}^{l'} \beta_{pq}^{ij} \varphi_{pq}(x_i, x_j) \tag{28}$$

where  $k, l, l'$  are the integers,  $\alpha_r^i, \beta_{pq}^{ij}$  are the constant coefficients to be determined,  $\varphi_r(x_i)$  and  $\varphi_{pq}(x_i, x_j)$  are the one- and two-variable basis functions. With these formulas, Eq. (14) can be approximated as

$$\hat{f}(\mathbf{x}) = f_0 + \sum_{i=1}^M \sum_{r=1}^k \alpha_r^i \varphi_r(x_i) + \sum_{1 \leq i < j \leq M} \sum_{p=1}^l \sum_{q=1}^{l'} \beta_{pq}^{ij} \varphi_{pq}(x_i, x_j) + \dots \tag{29}$$

We have employed the solution to evaluate the coefficient of orthonormal polynomials from the reference given in [44].

#### 4.4. Sampling

The generation of sample points is crucial for construction of the RS-HDMR based surrogate model. The quality of sample points governs the rate of convergence of Monte Carlo simulation, which is used to construct the component functions of RS-HDMR [45]. Quasi-random sample points are generated using the joint probability distribution of the input parameter [45]. Each sample point is chosen independently of all other sample points. In this work, quasi-random sequences are used to generate random sample points. These are totally deterministic and having low discrepancy. This ensures a more uniform distribution of sample points in the input domain compared to pseudo-random sample points, thus attaining faster convergence. The best known quasi-random points are Halton sequence [46], Sobol's sequence [30,31] and Faure sequence [47]. Sobol's sequence [30,31] exhibits better convergence than either Faure or Halton sequence [48].

#### 4.5. Summary of the proposed methodology

Based on the discussion so far, the proposed methodology for the RS-HDMR approximation is easily implemented using the following steps:

1. Identify the range of variability of the parametric Fuzzy variables.
2. Generate samples ( $N$ ) for fuzzy input parameters from Sobol's sequence [30,31].
3. Estimate the responses at all these sample points.
4. Determine  $f_0, f_i(x_i), f_{ij}(x_i, x_j)$  using Eqs. (24) and (28), respectively, using orthonormal polynomial basis functions.
5. Construct first- and second-order RS-HDMR approximation, respectively, using the following steps:

$$\hat{f}(\mathbf{x}) = f_0 + \sum_{i=1}^M \sum_{r=1}^k \alpha_r^i \varphi_r(x_i) \tag{30}$$

$$\hat{f}(\mathbf{x}) = f_0 + \sum_{i=1}^M \sum_{r=1}^k \alpha_r^i \varphi_r(x_i) + \sum_{1 \leq i < j \leq M} \sum_{p=1}^l \sum_{q=1}^{l'} \beta_{pq}^{ij} \varphi_{pq}(x_i, x_j) \tag{31}$$

6. Perform Monte Carlo simulation on the approximated response function  $\hat{f}(\mathbf{x})$  using uniform variables. Estimate the minimum–maximum range of the response for the particular  $\alpha$ -cut.
7. Repeat the procedure for different  $\alpha$ -cuts.

## 5. Numerical examples

The implementation of the RS-HDMR approach in fuzzy analysis is illustrated with the help of three examples in this section. When comparing computational efforts in evaluating the response intervals, the number of actual FE analyses is chosen as the primary comparison tool because this indirectly indicates the CPU time usage. For full scale MCS, the number of original FE analyses is same as the sample size. When the responses are evaluated through full scale MCS, the CPU time is higher since a number of repeated FE analysis are required. However, in the proposed method MCS is conducted within the proposed framework. Although the same sample size as for direct MCS is considered, the number of FE analyses is much lower. Hence, the computational effort expressed in terms of FE calculation alone should be carefully interpreted. Since the RS-HDMR approximation leads to an explicit representation of the system responses, the MCS can be conducted for any sample size. Sample required for RS-HDMR construction are generated from Sobol's sequence [30].

### 5.1. Example 1: modal analysis of a simplified aircraft wing

This example involves the estimation of bounds of the natural frequencies of a vibrating aircraft wing with length  $L_y = 1$  m and width  $L_z = 0.5$  m, as shown in Fig. 1. The mass of the engine is attached to the plate, which represents the wing, through a spring at one-third distance from the root of the wing. Poisson's ratio for the plate is taken as 0.33. The mass of the engine is taken as 0.80 times the mass of the wing. The stiffness of the spring is calculated from the second natural frequency of the wing. The thickness, mass density and elastic modulus of the wing are taken as fuzzy variables. The bounds of the variables are tabulated in Table 1. The response quantities, which are the natural frequencies of the wing structure, are represented by an RS-HDMR expansion. Note that in this example, the responses (natural frequencies) are monotonic functions of the parameters. Furthermore, there is no nonproportional damping, mode crossing or veering in the parameter range considered, where eigensolutions can be extremely sensitive to the parameters [50]. The proposed approach with RS-HDMR approximation and full scale MCS using the commercial FE code ADINA [49] are employed to evaluate the fuzzy characteristics of the natural frequencies of the structure. Therefore, computational efficiency, even for this simplified model, is a major practical requirement in solving the dynamic system. Using samples generated for the RS-HDMR, approximation errors (compared with full scale MCS) in the response bounds are presented in Fig. 2. The errors in the response bounds at  $\alpha$ -cuts of 0 and 0.2 are quite high ( $\approx 3$ –6%), however, these errors can be reduced by taking more RS-HDMR sample points (increase  $N$ ), which demands more FE analyses. Thus, the number of sample points ( $N$ ) for the RS-HDMR approximation will vary depending on the user's accuracy requirement. The full scale MCS results are obtained from  $10^5$  FE analyses. In contrast, only 256 (input sample for fuzzy parameters are generated from Sobol's sequence [30]) FE analyses are required by RS-HDMR for each  $\alpha$ -cut. In this problem, for each  $\alpha$ -cut, the total CPU usage for full scale MCS is 10 001 s, whereas for HDMR approximation it is only 46 s.

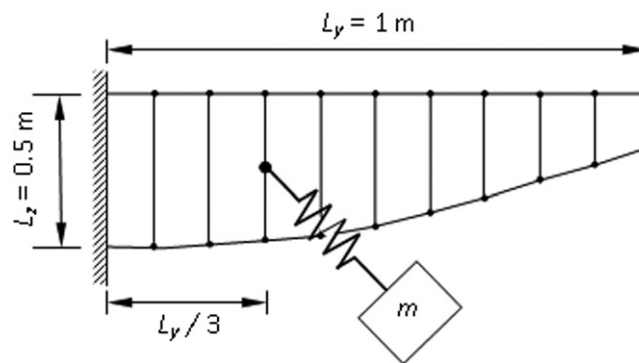


**Fig. 1.** The finite element model of a simplified aircraft wing with the engine modeled as a lumped mass attached to the wing via a spring at 1/3 span. The structure is modeled in the ADINA [49] FE software. The  $10 \times 5$  FE model of the plate consists of 50 2-D solid elements and 303 nodes. A fixed boundary condition is applied at the left.

**Table 1**  
Bounds of the input fuzzy variables of Example 1 at  $\alpha$ -cut = 0.

Variable	$x_{min}$	$x_{max}$
Young's modulus (GPa)	29	109
Thickness (m)	0.1	0.5
Density ( $\text{kg/m}^3$ )	2000	4000



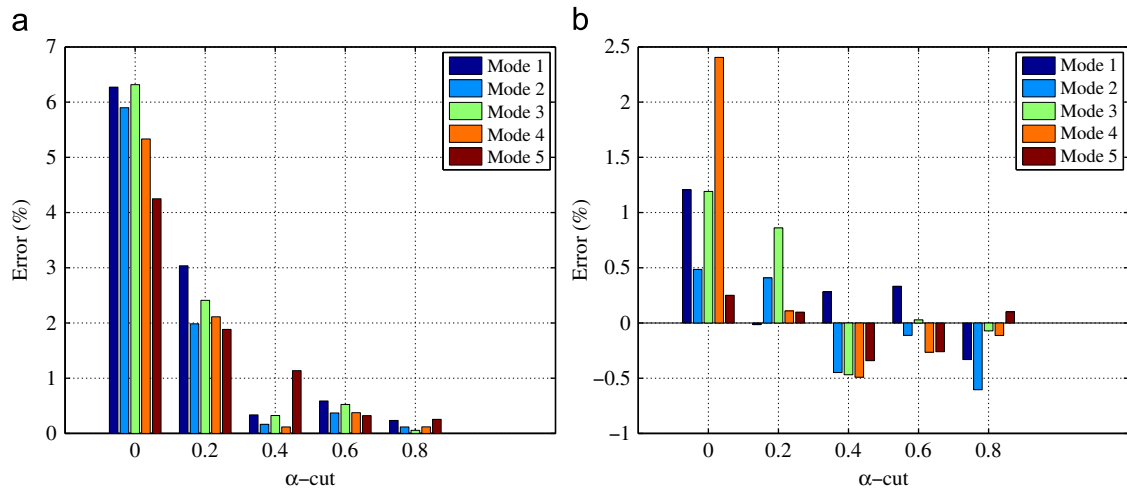


Fig. 2. Errors in the response bounds of the natural frequencies using proposed RS-HDMR based approach compared to MCS: (a) errors in the lower bounds and (b) errors in the upper bounds.

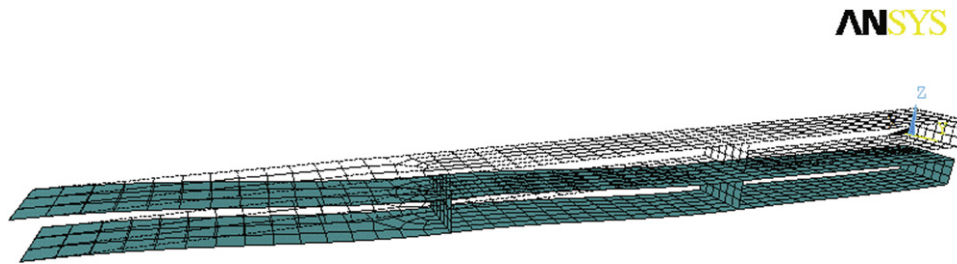


Fig. 3. The finite element model of a cantilever box beam. The structure is modeled in the ANSYS [51] FE software.

Table 2

First eight frequencies of the cantilever box beam (Fig. 3).

	1	2	3	4	5	6	7	8
Frequencies (Hz)	0.803	2.485	4.103	8.776	9.752	10.576	10.711	12.519

### 5.2. Example 2: modal analysis of a cantilever box beam

Consider the cantilevered box beam [25] shown in Fig. 3. This structure is composed of 5 plates and modelled with 516 shell elements (SHELL 63) and 3624 degrees of freedom in the commercial FE code ANSYS [51]. Its material properties are Youngs modulus  $E = 72 \times 10^4 \text{ N/m}^2$ , Poisson's ratio  $\nu = 0.3$ , and density  $\rho = 2700 \text{ kg/m}^3$ . Its overall geometric characteristics are length  $L = 3 \text{ m}$ , width  $l = 0.2 \text{ m}$ , and height  $h = 0.1 \text{ m}$ , with the individual plates  $e$  being 2 mm thick. The first eight frequencies of the structure are presented in Table 2, which is in excellent agreement with previous results [25]. These frequencies constitute the initial data for the parametric study. The parametric study has been performed considering 20% variation of the plate thickness. Five fuzzy parameters are defined, and the variation of eight frequencies of the structures are calculated. Using samples generated for the RS-HDMR, approximation errors (compared with full scale MCS) in the lower and upper bounds for the frequencies is shown in Fig. 4. The full scale MCS results are obtained from  $10^5$  FE analyses. In contrast, only 256 (input sample for fuzzy parameters are generated from Sobol's sequence [30]) FE analyses are required by RS-HDMR. The results obtained using HDMR-based approach are very close to the reference data obtained with Zadeh's Extension Principle [7,25]; the maximum error in the calculations of the lower and upper modal quantities is on the order of 0.2%. Fig. 4 shows an excellent agreement of the results obtained using the present approach with the available results [25]. In general, the percentage error is significantly lower compared to Example 1. The higher error for the lower values of  $\alpha$ -cut in Example 1 can be attributed to relatively higher parametric variability as given in Table 1.

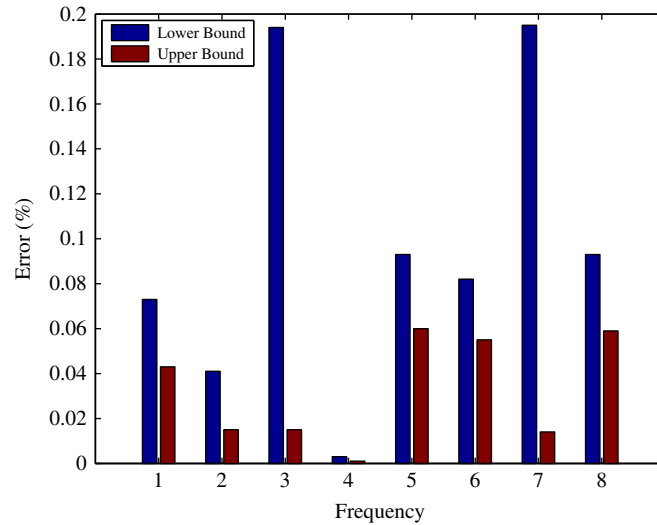


**Fig. 4.** Comparison of the lower and upper bound errors of estimated frequencies using full scale MCS with  $10^5$  FE analyses and present approach for  $\alpha$ -cut = 0.

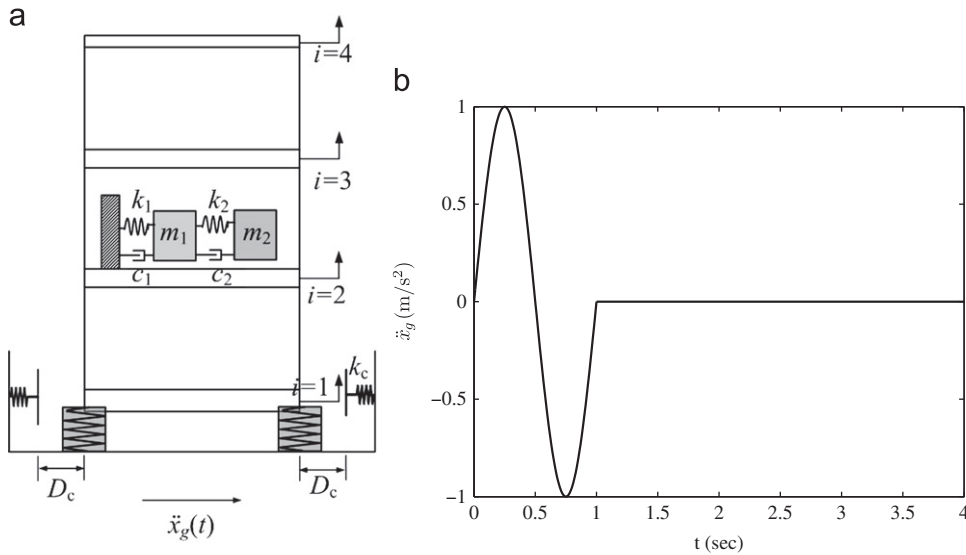


**Fig. 5.** Problem statement (Example 3): (a) base isolated structure with an equipment isolation system on the second floor and (b) acceleration history.

### 5.3. Example 3: time-domain response of a six degrees of freedom system dynamical system

This example considers a four-storey building excited by a single period sinusoidal pulse of ground motion, studied by Gavin and Yau [52]. Fig. 5(a) shows the four-storey building with isolation systems and Fig. 5(b) presents the acceleration history. The building contains isolated equipment resting on the second floor. The motion of the ground floor is resisted mainly by base isolation bearings [52] and if its displacement exceeds  $D_c (= 0.50$  m) then an additional stiffness force contributes to the resistance. The Mass, stiffness and damping coefficients,  $m_f$ ,  $k_f$  and  $c_f$ , respectively, at each floor are assumed to be identical.

There are two isolated masses, representing isolated, shock-sensitive equipment resting on the second floor. The larger mass  $m_1 (= 500$  kg) is connected to the floor by a relatively flexible spring,  $k_1 (= 2500$  N/m), and a damper,  $c_1 (= 350$  N/m/s), representing the isolation system. The smaller mass  $m_2 (= 100$  kg) is connected to the larger mass by a relatively stiff spring,  $k_2 (= 10^5$  N/m), and a damper,  $c_2 (= 200$  N/m/s), representing the equipment itself. Descriptions of the fuzzy variables are listed in Table 3. The limit state is defined by the combination of three failure modes leading to

**Table 3**  
Description and bounds of the input fuzzy variables of Example 3 at  $\alpha$ -cut = 0.

Variable	Description	Units	$x_{min}$	$x_{max}$
$m_f$	Floor mass	kg	4200	7800
$k_f$	Floor stiffness	N/m	$2.1 \times 10^7$	$3.9 \times 10^7$
$c_f$	Floor damping coefficient	N/m/s	24000	96000
$d_y$	Isolation yield displacement	m	0.02	0.08
$f_y$	Isolation yield force	N	8000	32000
$d_c$	Isolation contact displacement	m	0.35	0.65
$k_c$	Isolation contact stiffness	N	$2.1 \times 10^7$	$5.7 \times 10^7$
$m_1$	Mass of Block 1	kg	400	800
$m_2$	Mass of Block 2	kg	80	160
$k_1$	Stiffness of Spring 1	N/m	2000	4000
$k_2$	Stiffness of Spring 2	N/m	$8.0 \times 10^4$	$1.60 \times 10^5$
$c_1$	Damping coefficient of damper 1	N/m/s	343	371
$c_2$	Damping coefficient of damper 2	N/m/s	196	212
$T$	Pulse excitation period	s	0.8	1.6
$A$	Pulse amplitude	m/s/s	0.50	2.50

**Table 4**  
Comparison of response bounds obtained from RS-HDMR approximation and MCS in Example 3.

$\alpha$ -Cut	Methods	$N=64$		$N=128$		$N=256$	
		$f_{min}$	$f_{max}$	$f_{min}$	$f_{max}$	$f_{min}$	$f_{max}$
0.0	RS-HDMR	-3.45182	1.28165	-3.67887	1.21043	-3.73127	1.18103
	MCS	-3.73387	1.17023	-3.73387	1.17023	-3.73387	1.17023
	% error	7.55	-9.52	1.47	-3.44	0.07	-0.92
0.2	RS-HDMR	-2.24593	0.70095	-2.20879	0.71968	-2.17188	0.71999
	MCS	-2.17684	0.72059	-2.17684	0.72059	-2.17684	0.72059
	% error	-3.17	2.72	-1.47	0.13	0.23	0.08
0.4	RS-HDMR	-0.98498	-0.02321	-0.97010	0.02028	-0.96219	-0.02021
	MCS	-0.96237	-0.02012	-0.96237	-0.02012	-0.96237	-0.02012
	% error	-2.35	-15.35	-0.80	-0.79	0.02	-0.45

system failure and has the following form:

$$f(\mathbf{x}) = 12.50 \left( 0.04 - \max_t |x_{f_i}(t) - x_{f_{i-1}}(t)| \right)_{i=2,3,4} + \left( 0.50 - \max_t |\ddot{x}_g(t) + \ddot{x}_{m_2}(t)| \right) + 2.0 \left( 0.25 - \max_t |x_{f_2}(t) - x_{m_1}(t)| \right) \quad (32)$$

where  $x_{f_i}(t)$  refers to the displacement of  $i$ th floor and  $(x_{f_i}(t) - x_{f_{i-1}}(t))$  is the inter-storey drift.  $\ddot{x}_g(t)$  is the ground acceleration and  $\ddot{x}_{m_2}(t)$  is the acceleration of the smaller mass block. The displacement of the larger mass block is  $x_{m_1}(t)$  and represents the displacement of the equipment isolation system. The limit state in Eq. (32) is the overall representation of three failure modes. The first term describes the damage to the structural system due to excessive deformation. The second term represents the damage to equipment caused by excessive acceleration. The last term represents the damage of the isolation system. The weighing factors, multiplied with each term in Eq. (32), are mainly to emphasize the equal contribution of the individual failure modes to the overall failure of system. It is desirable that (a) inter-storey drift is limited to 0.04 m, (b) the peak acceleration of the equipment is less than 0.50 m/s<sup>2</sup>, and (c) the displacement across the equipment isolation system is less than 0.25 m. Eq. (32) signifies overall system failure, which does not necessarily occur when one or two of the above mentioned failure criteria is satisfied.

Similar to the previous example, the approximate response function is constructed by generated sample points according to Sobol’s sequence [30,31]. Table 4 compares the results obtained by the present method using the RS-HDMR approximation with direct MCS using uniform variables with specified limits. A sampling size  $N_S = 10^5$  is considered in direct MCS to compute the response bounds. A similar analysis is performed for different  $\alpha$ -cuts and presented in Table 4. The total number of function calls for each  $\alpha$ -cut is 256. It is evident that the total number of original function evaluations is significantly less compared to the direct simulation.

### 6. Conclusions

Structural dynamics analysis with fuzzy uncertain variables is considered. A novel Random Sampling High-Dimensional Model Representation (RS-HDMR) method for multivariate function approximation is suggested for this purpose. HDMR is

a general set of fully functional operational model for high-dimensional input–output systems. When data are arbitrary spaced in the input domain, RS-HDMR can be constructed. The RS-HDMR component functions involve high-dimensional integrals that may be approximately calculated by Monte Carlo integration. Because the direct determination of high-order RS-HDMR component functions by Monte Carlo integration is prohibitively expensive, analytical basis functions are employed to approximate RS-HDMR component functions. With such basis functions, only one set of input samples of the output is needed to determine all RS-HDMR component functions. Thus, the sampling effort is dramatically reduced.

The RS-HDMR method is applied to different  $\alpha$ -cuts to obtain the fuzzy description of the output variables. Three numerical examples show the performance of the proposed method. Comparisons are made with the full scale simulation to evaluate the accuracy and computational efficiency of the proposed method. These numerical examples show that the proposed method not only yields accurate estimates of the response bounds compared to the direct simulation approach, but also reduces the computational effort significantly. Due to a small number of original function evaluations, the proposed RS-HDMR approximations are very effective, particularly when a response evaluation entails costly finite element analysis, or other computationally expensive numerical methods. In order to reduce the approximation error further, a second-order RS-HDMR approximation could be used, but the number of function evaluations would be increased quadratically. An optimum number of sample points,  $N$ , must be chosen in the function approximation by the RS-HDMR, depending on the desired accuracy and computational resources.

The error using RS-HDMR tends to decrease significantly with increasing number of sample points (e.g., as the intervals become smaller). However, the computed error does not go to zero as the intervals become smaller. This is because the RS-HDMR approximations are essentially built on truncated series. Thus, there will always be some truncation error, irrespective of number of sample points considered. The computational efficiency of the approach is more difficult to quantify as this depends on the details of the method used to obtain the response bounds of the full system. However, the RS-HDMR approximation may be used either on its own or in collaboration with a full system optimization. In this discussion, we will assume that the only significant computational burden is calculating the response of the full model. There is a second use of the RS-HDMR approach. Although the results are only approximate, the RS-HDMR optimal parameters will be close to the optimal parameters of the full system. Thus, the RS-HDMR approximation can be used to determine the parameter vertices that are likely to lead to the extreme responses, identify the boundaries in parameter space for further investigation, or provide initial estimates of interior points in parameter space that are likely to give extreme responses.

## Acknowledgements

R.C. and S.A. acknowledge the support of Royal Society through the award of Newton International Fellowship and Wolfson Research Merit award respectively.

## References

- [1] R. Ghanem, P. Spanos, *Stochastic Finite Elements: A Spectral Approach*, Springer-Verlag, New York, USA, 1991.
- [2] B. Sudret, A. Der-Kiureghian, *Stochastic Finite Element Methods and Reliability*, Technical Report UCB/SEMM-2000/08, Department of Civil & Environmental Engineering, University of California, Berkeley, November 2000.
- [3] R. Chowdhury, S. Adhikari, High dimensional model representation for stochastic finite element analysis, *Appl. Math. Modell.* 34 (12) (2010) 3917–3932.
- [4] P.B. Nair, A.J. Keane, Stochastic reduced basis methods, *AIAA J.* 40 (8) (2002) 1653–1664.
- [5] R.E. Moore, *Interval Analysis*, Prentice-Hall, Englewood Cliffs, NJ, USA, 1966.
- [6] Y.B. Haim, I. Elishakoff, *Convex Models of Uncertainty in Applied Mechanics*, Elsevier, Amsterdam, 1990.
- [7] L.A. Zadeh, Fuzzy sets, *Inf. Control* 8 (3) (1965) 338–353.
- [8] D. Moens, D. Vandepitte, Recent advances in non-probabilistic approaches for non-deterministic dynamic finite element analysis, *Arch. Comput. Methods Eng.* 13 (3) (2006) 389–464.
- [9] D. Moens, D. Vandepitte, A survey of non-probabilistic uncertainty treatment in finite element analysis, *Comput. Methods Appl. Mech. Eng.* 194 (12–16) (2005) 1527–1555.
- [10] B. Mace, K. Worden, G. Manson, Uncertainty in structural dynamics, *J. Sound Vib.* 288 (3) (2005) 423–429.
- [11] G. Manson, Calculating frequency response functions for uncertain systems using complex affine analysis, *J. Sound Vib.* 288 (3) (2005) 487–521.
- [12] D. Degrauwe, G. Lombaert, G.D. Roeck, Improving interval analysis in finite element calculations by means of affine arithmetic, *Comput. Struct.* 88 (3–4) (2010) 247–254.
- [13] Z. Qiu, X. Wang, M. Friswell, Eigenvalue bounds of structures with uncertain-but-bounded parameters, *J. Sound Vib.* 282 (1–2) (2005) 297–312.
- [14] B. Lallemand, G. Plessis, T. Tison, P. Level, Neumann expansion for fuzzy finite element analysis, *Eng. Comput.* 16 (5) (1999) 572–583.
- [15] O. Giannini, M. Hanss, The component mode transformation method: a fast implementation of fuzzy arithmetic for uncertainty management in structural dynamics, *J. Sound Vib.* 311 (3–5) (2008) 1340–1357.
- [16] M. Hanss, The transformation method for the simulation and analysis of systems with uncertain parameters, *Fuzzy Sets Syst.* 130 (3) (2002) 277–289.
- [17] M. Hanss, The extended transformation method for the simulation and analysis of fuzzy-parameterized models, *Int. J. Uncertainty Fuzziness Knowl.-Based Syst.* 11 (6) (2003) 711–727.
- [18] U. Gauger, S. Turrin, M. Hanss, L. Gaul, A new uncertainty analysis for the transformation method, *Fuzzy Sets Syst.* 159 (11) (2008) 1273–1291.
- [19] M. De Munck, D. Moens, W. Desmet, D. Vandepitte, An efficient response surface based optimisation method for non-deterministic harmonic and transient dynamic analysis, *CMES—Comput. Model. Eng. Sci.* 47 (2) (2009) 119–166.
- [20] M. De Munck, D. Moens, W. Desmet, D. Vandepitte, A response surface based optimisation algorithm for the calculation of fuzzy envelope FRFs of models with uncertain properties, *Comput. Struct.* 86 (10) (2008) 1080–1092.

- [21] D. Moens, D. Vandepitte, A fuzzy finite element procedure for the calculation of uncertain frequency-response functions of damped structures: part 1—procedure, *J. Sound Vib.* 288 (3) (2005) 431–462.
- [22] H. De Gerssem, D. Moens, W. Desmet, D. Vandepitte, A fuzzy finite element procedure for the calculation of uncertain frequency response functions of damped structures: part 2—numerical case studies, *J. Sound Vib.* 288 (3) (2005) 463–486.
- [23] D. Moens, D. Vandepitte, Fuzzy finite element method for frequency response function analysis of uncertain structures, *AIAA J.* 40 (1) (2002) 126–136.
- [24] F. Massa, T. Tison, B. Lallemand, Fuzzy modal analysis: prediction of experimental behaviours, *J. Sound Vib.* 322 (1–2) (2009) 135–154.
- [25] F. Massa, K. Ruffin, T. Tison, B. Lallemand, A complete method for efficient fuzzy modal analysis, *J. Sound Vib.* 309 (1–2) (2008) 63–85.
- [26] F. Massa, B. Lallemand, T. Tison, P. Level, Fuzzy eigensolutions of mechanical structures, *Eng. Comput.* 21 (1) (2004) 66–77.
- [27] G. Plessis, B. Lallemand, T. Tison, P. Level, Fuzzy modal parameters, *J. Sound Vib.* 233 (5) (2000) 797–812.
- [28] G. Li, C. Rosenthal, H. Rabitz, High dimensional model representations, *J. Phys. Chem. A* 105 (33) (2001) 7765–7777.
- [29] S. Adhikari, R. Chowdhury, M.I. Friswell, High dimensional model representation method for fuzzy structural dynamics, *J. Sound Vib.* 330 (7) (2011) 1516–1529.
- [30] P. Bratley, B.L. Fox, Implementing Sobol's quasirandom sequence generator, *ACM Trans. Math. Software* 14 (1) (1988) 88–100.
- [31] I.M. Sobol, Uniformly distributed sequences with an additional uniform property, *USSR Comput. Math. Math. Phys.* 16 (1976) 236–242.
- [32] M. De Munck, D. Moens, W. Desmet, D. Vandepitte, An adaptive Kriging based optimisation algorithm for interval and fuzzy FRF analysis, in: *Proceedings of ISMA 2008: International Conference on Noise and Vibration Engineering*, vols. 1–8, 2008, pp. 3767–3776.
- [33] R. Chowdhury, B.N. Rao, A.M. Prasad, Stochastic sensitivity analysis using HDMR and score function, *Proc. Indian Acad. Eng. Sci.* 34 (6) (2009) 967–986.
- [34] G. Li, S. Wang, H. Rabitz, Practical approaches to construct RS-HDMR component functions, *J. Phys. Chem. A* 106 (37) (2002) 8721–8733.
- [35] I. Sobol, Theorems and examples on high dimensional model representation, *Reliab. Eng. Syst. Safety* 79 (2) (2003) 187–193.
- [36] R. Chowdhury, B.N. Rao, A.M. Prasad, High-dimensional model representation for structural reliability analysis, *Commun. Numer. Methods Eng.* 25 (4) (2009) 301–337.
- [37] J. Shorter, P. Ip, H. Rabitz, An efficient chemical kinetics solver using high dimensional model representation, *J. Phys. Chem. A* 103 (36) (1999) 7192–7198.
- [38] R. Chowdhury, B.N. Rao, Assessment of high dimensional model representation techniques for reliability analysis, *Probab. Eng. Mech.* 24 (1) (2009) 100–115.
- [39] G. Li, S. Wang, H. Rabitz, S. Wang, P. Jaffe, Global uncertainty assessments by high dimensional model representations (HDMR), *Chem. Eng. Sci.* 57 (21) (2002) 4445–4460.
- [40] B.N. Rao, R. Chowdhury, Factorized high dimensional model representation for structural reliability analysis, *Eng. Comput.* 25 (7–8) (2008) 708–738.
- [41] B.N. Rao, R. Chowdhury, Enhanced high-dimensional model representation for reliability analysis, *Int. J. Numer. Methods Eng.* 77 (5) (2009) 719–750.
- [42] Y. Yaman, M. Demiralp, A new rational approximation technique based on transformational high dimensional model representation, *Numer. Algorithms* 52 (3) (2009) 385–407.
- [43] R. Chowdhury, B.N. Rao, Hybrid high dimensional model representation for reliability analysis, *Comput. Methods Appl. Mech. Eng.* 198 (5–8) (2009) 753–765.
- [44] L. Genyuan, R. Herschel, H. Jishan, C. Zheng, J. Yiguang, Regularized random-sampling high dimensional model representation (RS-HDMR), *J. Math. Chem.* 43 (3) (2008) 1207–1232.
- [45] H. Niederreiter, *Random Number Generation and Quasi-Monte Carlo Methods*, Society for Industrial and Applied Mathematics, Philadelphia, PA, USA, 1992.
- [46] J.H. Halton, On the efficiency of certain quasi-random sequences of points in evaluating multi-dimensional integrals, *Numer. Math.* 2 (1960) 84–90.
- [47] H. Faure, Good permutations for extreme discrepancy, *J. Number Theory* 42 (1) (1992) 47–56.
- [48] S. Galanti, A. Jung, Low-discrepancy sequences: Monte Carlo simulation of option prices, *J. Derivatives* 5 (1) (1997) 63–83.
- [49] *ADINA Theory and Modeling Guide*, ADINA R & D, Inc., Report ARD 05-6, 2005.
- [50] S. Adhikari, Calculation of derivative of complex modes using classical normal modes, *Comput. Struct.* 77 (6) (2000) 625–633.
- [51] ANSYS Inc., *Mechanical APDL Theory Manual*, 2011.
- [52] H.P. Gavin, S.C. Yau, High-order limit state functions in the response surface method for structural reliability analysis, *Struct. Safety* 30 (2) (2008) 162–179.